

# 高誘電率ゲート酸化膜を用いた電界効果トランジスタによる 有機薄膜の物性変調

## Modification of physical properties of an organic thin film using a field effect transistor fabricated on a high-*k* gate oxide film

上野 啓司 (理学部基礎化学科 助教授)

Keiji Ueno (Associate Professor, Department of Chemistry, Faculty of Science)

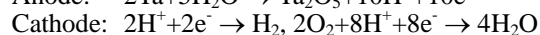
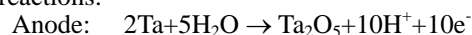
### I. INTRODUCTION

Recently, organic field effect transistors (OFETs) have been widely studied not only for technological applications, but also for modification of the organic material properties through 'physical doping' instead of 'chemical doping'.<sup>1,2</sup> In the case of chemical doping, it is difficult to finely control the amount of the carrier injection, and it is impossible to change the polarity of the carrier without changing the doping material. During the physical doping, carriers are injected into the organic active layer by applying a high bias voltage to the gate electrode, and the number of injected carriers is proportional to the applied gate voltage times the capacitance of the gate capacitor. Therefore, it is possible to control the amount and the polarity of the injected carriers by only changing the gate voltage. Of course, the actual behavior of the physical carrier injection is strongly affected by the electronic properties of the OFET components.<sup>3,4</sup>

In order to inject more carriers into the organic layer, applying a high voltage to the gate electrode, or utilizing a gate insulator having a high dielectric constant is required. In many cases OFETs have been fabricated on thermally oxidized SiO<sub>2</sub> surfaces of heavily doped conductive Si substrates. Although SiO<sub>2</sub> is a good insulator and has a very high dielectric strength, approximately 10 MV/cm, the dielectric constant of SiO<sub>2</sub>, however, is not very high, approximately 4. Thus, many groups have been trying to fabricate an OFET on a high-*k* (high dielectric constant) gate insulator to inject more carriers. Another advantage of high-*k* materials is a lower working voltage.<sup>5-10</sup> In the present study, we focused on tantalum (V) oxide (Ta<sub>2</sub>O<sub>5</sub>) from among the various high-*k* materials. The dielectric constant of Ta<sub>2</sub>O<sub>5</sub> is approximately 25 ~ 27, and it has a rather high dielectric strength, 5 MV/cm at best.<sup>11</sup> Therefore, it will be possible to inject more than 3 times a higher amount of carriers into the organic layer on Ta<sub>2</sub>O<sub>5</sub> than on SiO<sub>2</sub> if the thickness of the dielectrics is same, and the best dielectric breakdown characteristics are really achieved.

It is difficult, however, to fabricate a good Ta<sub>2</sub>O<sub>5</sub> film with a high dielectric strength and a smooth surface on which a good organic film could be grown. In many cases, high-*k* metal oxide films are grown by the e-beam evaporation,<sup>9</sup> sputtering,<sup>10</sup> chemical vapor deposition, or laser-ablated molecular beam epitaxy (MBE) method, but they require expensive equipment and highly complicated techniques to

grow a stoichiometric, low-defect smooth film. Instead, we tried to fabricate a Ta<sub>2</sub>O<sub>5</sub> film using the anodic oxidation (anodization) method, which requires no vacuum apparatus or high-temperature process.<sup>12-14</sup> In this method, a Ta<sub>2</sub>O<sub>5</sub> film grows on the Ta surface by the following electrochemical reactions:



During the anodization, growth of the Ta<sub>2</sub>O<sub>5</sub> film proceeds under 'negative feedback' conditions. Namely, more electrochemical current flows at thinner or defective parts in the growing oxide film, so that these defects are automatically restored. In this process, the flatness of the Ta sheet is essential to achieve a sufficiently smooth Ta<sub>2</sub>O<sub>5</sub> surface. In previous reports, thin Ta films deposited on flat substrate surfaces were utilized as the smooth surface.<sup>6-8</sup> Instead, we tried to produce a smooth surface on a commercially available Ta sheet by electrolytic polishing. As described later, it was found that this polishing process is fundamental for making a good Ta<sub>2</sub>O<sub>5</sub> film having a superior dielectric strength.

On the anodized Ta<sub>2</sub>O<sub>5</sub>/Ta gate substrates, we fabricated bottom-gate type OFETs using pentacene and C<sub>60</sub>, which show p-type and n-type working characteristics,<sup>2</sup> respectively. It has been found that both types of OFETs work well, and the pentacene OFET showed as high a mobility as that on the SiO<sub>2</sub>/Si bottom gate. In this paper, we mainly report the fabrication process of the Ta<sub>2</sub>O<sub>5</sub>/Ta bottom gate and its dielectric breakdown properties together with the working characteristics of the OFETs.

### II. EXPERIMENTAL

The specimen was cut from a commercially available 99.99% purity, 0.1 mm-thick Ta sheet purchased from Furuuchi Kagaku Co., Ltd. It was degreased in acetone, rinsed in ultrapure water, and subjected to electrolytic polishing. A mixture of conc. H<sub>2</sub>SO<sub>4</sub> and 50% aqueous HF solution with a 9:1 volumetric ratio was used as the electrolyte. The Ta anode and a SUS304 cathode were dipped in the stirred electrolyte about 4 cm apart, and a regulated DC 20 V was applied to the electrodes. After a 5-minute electrolysis, the substrate was washed in 10% aqueous HF solution, rinsed in ultrapure water and dried by flowing N<sub>2</sub> gas. The electrolysis, washing and drying processes were repeated until a mirror-like Ta surface was obtained. Usually 20

repetitions were required to produce a good surface.

After the electrolytic polishing, the Ta substrate was anodized in an aqueous KI solution with a concentration of  $2 \times 10^{-4}$  mol/l. A Ta sheet was used as the cathode, and two electrodes were set 2 cm apart in a 100 ml beaker containing the KI solution. The beaker was set in an ultrasonic bath to eliminate air bubbles sometimes generated around the anode surface. The anode voltage was increased at a rate of 0.25 V/s up to the final anodizing voltage (100 ~ 350 V), and then kept constant. The anodizing current gradually decreased under the application of a constant voltage due to the growth of the insulating Ta<sub>2</sub>O<sub>5</sub> layer. The anodization was continued until the current decreased to lower than the preset value (1 ~ 10  $\mu$ A/cm<sup>2</sup>). The sample was then rinsed in ultrapure water, and dried by flowing N<sub>2</sub> gas. The thickness of the anodized Ta<sub>2</sub>O<sub>5</sub> layer was estimated by capacitance measurements using an LCR meter (Protek Z9216), and by optical reflectance spectroscopy.

KI was chosen as the electrolyte for the anodization because the iodide ion (I<sup>-</sup>) has a larger ion radius, and smaller bond energy with the Ta cation. Therefore, it was expected that iodine would be hardly incorporated into the anodized Ta<sub>2</sub>O<sub>5</sub> film during the electrochemical reaction. Actually, no trace of potassium or iodine was found in the Ta<sub>2</sub>O<sub>5</sub> film anodized in the KI solution, which was confirmed by X-ray photoelectron spectroscopy (XPS). XPS also proved the stoichiometry of the Ta<sub>2</sub>O<sub>5</sub> film within its accuracy.

Figure 1 shows the structure of the OFET fabricated on the Ta<sub>2</sub>O<sub>5</sub>/Ta bottom gate substrate. Organic semiconductors, pentacene (Aldrich, 98%) and C<sub>60</sub> (99.99%) were deposited from Knudsen cells onto the Ta<sub>2</sub>O<sub>5</sub> surface at room temperature in an ultrahigh vacuum MBE chamber. The deposition rate and the thickness were set at 1 nm/min and 100 nm, respectively. The morphology and crystallinity of the organic films on the Ta<sub>2</sub>O<sub>5</sub> surfaces were investigated by X-ray diffraction (XRD) and atomic force microscopy (AFM). In the FET measurement, the source and drain electrodes of Au were formed by vapor deposition through a metal shadow mask on top of the organic layer. The channel width and length were 1 mm and 0.1 mm, respectively. These OFET characteristics were measured using two picoammeter/voltage sources (Keithley Model 6487). The pentacene OFETs were characterized in a vacuum desiccator evacuated by a rotary pump after the wiring, while the C<sub>60</sub> OFETs were introduced into an ultra-high vacuum chamber after the wiring, heated at 150°C under a vacuum pressure of 10<sup>-7</sup> Pa for several hours, and characterized under the high vacuum pressure of 10<sup>-4</sup> Pa to eliminate the influence of oxygen adsorption.

### III. RESULTS AND DISCUSSION

Figure 2 shows AFM images of a Ta sheet before and after the electrolytic polishing and the

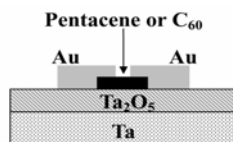


FIG. 1 Structure of a top-contact type organic FET fabricated on an anodized Ta<sub>2</sub>O<sub>5</sub> gate dielectric on a Ta sheet.

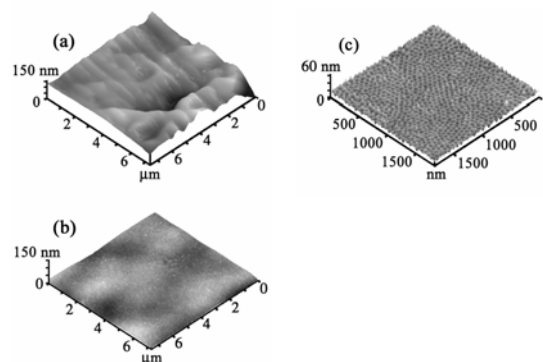


FIG. 2 AFM images of a Ta sheet before and after the electrolytic polishing in the mixture of aqueous HF and conc. H<sub>2</sub>SO<sub>4</sub>. (a) before the polishing, (b) after the polishing, and (c) an enlarged AFM image of the polished Ta surface.

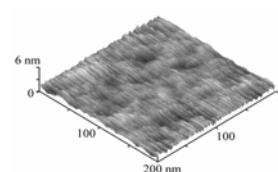


FIG. 3 An AFM image of the Ta surface after the electrolytic polishing and the anodization in a dilute HF aqueous solution.

anodization. As shown in Fig. 2(a), the Ta surface initially had a very high roughness due to the mechanical polishing or the rolling process. After the repeated electrolytic polishings, they were almost planed away and a very smooth surface seemed to be obtained as shown in Fig. 2(b). The root mean square (rms) values of the surface roughness were 18 nm and 6.3 nm for Fig. 2(a) and 2(b), respectively. A detailed AFM image of the electrolytically polished surface, however, revealed a highly porous surface as shown in Fig. 2(c), which is very similar to the porous alumina<sup>15</sup> or tantalum<sup>16</sup> surface anodized in an acid solution. The diameter of the pores was very uniform, about 20 nm, and their depth was greater than 10 nm, which could not be accurately measured by AFM due to the large curvature of the cantilever tip. The mechanism for the generation of these pores on the Ta surface during the electrochemical polishing is not fully understood and now under investigation.

After the anodization in the dilute KI solution, these pores completely diminished. Figure 3 shows an AFM image of the surface anodized at 300V until the anodic current became less than 10  $\mu$ A. At this voltage, the thickness of the oxidized Ta film was estimated to be 600 nm, which was verified by the optical reflection measurement. The rms roughness value of this surface was 0.13 nm, which is as low as that of the thermally oxidized SiO<sub>2</sub> surface on a Si substrate.

In order to check the breakdown voltage of the anodized Ta<sub>2</sub>O<sub>5</sub> films, capacitors were fabricated by evaporating Au electrodes on their surfaces, and a DC voltage was applied between the top Au and the base Ta electrodes. Figure 4 shows the I-V characteristics of Ta<sub>2</sub>O<sub>5</sub> capacitors with and without the electrolytic polishing of the Ta surfaces before the anodization. For both specimens, the Ta surfaces were anodized at 100 V to fabricate Ta<sub>2</sub>O<sub>5</sub> films as thick as 200 nm. The capacitor without polishing

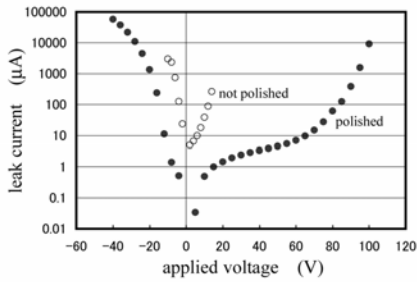


FIG. 4 I-V characteristics of  $\text{Ta}_2\text{O}_5$  films anodized at 100 V. Filled and open circles represent I-V curves of the  $\text{Ta}_2\text{O}_5$  films with and without the electrolytic polishing before the anodization, respectively.

revealed a very low breakdown voltage, while that on the polished Ta surface had a high breakdown voltage. Note that the breakdown voltage is far lower when the top Au is positively biased and the base Ta is negatively biased, which is the reverse of that during the anodization of the Ta surface. It is well known that a  $\text{Ta}_2\text{O}_5$  capacitor is very fragile and easily broken down when a reverse bias voltage is applied between the electrodes. For the present specimens, the maximum breakdown voltage under the forward bias condition was 100V leading to the dielectric strength of 5 MV/cm, which is better than the previously reported value of a thermally oxidized  $\text{Ta}_2\text{O}_5/\text{Ta}$  film.<sup>11</sup> In contrast, the dielectric strength was about 2 MV/cm under the reverse bias condition. Here, the dielectric constant of this capacitor calculated from the capacitance ( $124 \text{ nF/cm}^2$  at 1 KHz) and the optically measured thickness (200 nm) was about 28. So it is really expected that more than a three times larger amount of electrons can be ideally injected into the organic layer on the anodized  $\text{Ta}_2\text{O}_5$  gate capacitor than that on the thermally oxidized  $\text{SiO}_2/\text{Si}$  gate when the maximum positive bias voltage is applied to the gate electrode. Of course, appropriate source and drain electrode materials should be chosen and the well-ordered organic channel layer must be fabricated on the gate capacitor in order to inject such a high amount of carriers into the organic layer.<sup>3,4</sup> If a large injection barrier exists at the interface between the source or drain electrode and the organic layer, it is difficult to inject the ideal amount of carriers even if a very high gate voltage can be applied.

Using the  $\text{Ta}_2\text{O}_5/\text{Ta}$  substrates anodized at 300 V, we fabricated pentacene and  $\text{C}_{60}$  OFETs as shown in Fig. 1. Figure 5 shows an AFM image and an XRD pattern of a 100 nm pentacene film grown at room temperature on the anodized  $\text{Ta}_2\text{O}_5$  surface. The pentacene domains have very large dendritic structures, and the stacking structure of each unit layer is clearly observed. The XRD pattern revealed that the grown film has two types of c-axis ordering with the layer spacing of 1.42 nm and 1.51 nm, meaning that the pentacene film is a mixture of the so-called “thin film” and “bulk” phases.<sup>17</sup>

Figure 6 shows the drain current versus drain voltage characteristics of a p-type pentacene OFET as a function of the gate voltage. As shown in Fig. 6(b), this FET operates at low gate/drain voltages in the same manner as previous references<sup>5-10</sup>, due to the high dielectric constant of the  $\text{Ta}_2\text{O}_5$  gate material. In the present study, however, our main purpose is to

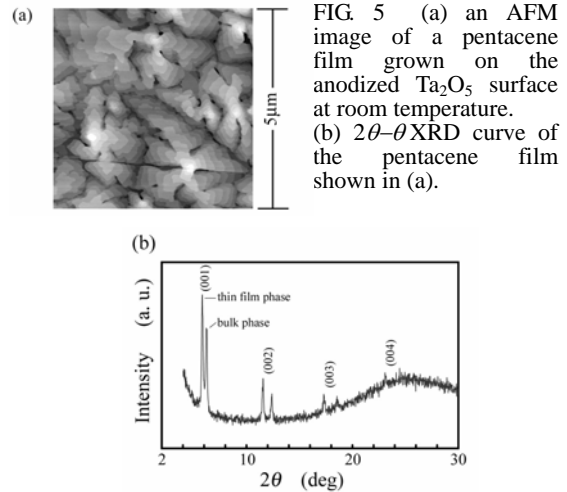


FIG. 5 (a) an AFM image of a pentacene film grown on the anodized  $\text{Ta}_2\text{O}_5$  surface at room temperature. (b)  $2\theta$ - $\theta$ XRD curve of the pentacene film shown in (a).

inject more and more carriers into the organic layer, and not to operate the FET at a low voltage. Thus, the high voltage operating characteristics will be mainly discussed. The mobility values of this FET in the linear region ( $V_D = -5\text{V}$ ) and in the saturated region ( $V_D = -90\text{V}$ ) were calculated to be  $0.35 \text{ cm}^2/\text{Vs}$  and  $0.20 \text{ cm}^2/\text{Vs}$ , respectively. The on-off ratio at  $V_D = -90\text{V}$  was about 4000. These mobility and on-off ratios were comparable with those of pentacene OFETs on  $\text{SiO}_2/\text{Si}$  gates, which were fabricated using the same sources and equipment. For the p-type FET, the reverse negative bias voltage is applied between the gate and source electrodes, corresponding to the reverse voltage to the anodized  $\text{Ta}_2\text{O}_5/\text{Ta}$  gate. Although quite a large leak current might flow between the gate and source electrodes, a far larger drain current due to the highly injected carriers conceals the leak current from the gate electrode, and typical FET characteristics can be obtained as shown in Fig. 6(a).

Figure 7 indicates the drain current versus drain voltage characteristics of an n-type  $\text{C}_{60}$  OFET as a function of the gate voltage. The  $\text{C}_{60}$  FET also operated at low gate/drain voltages (not shown). This result proves that the anodized  $\text{Ta}_2\text{O}_5/\text{Ta}$  gate

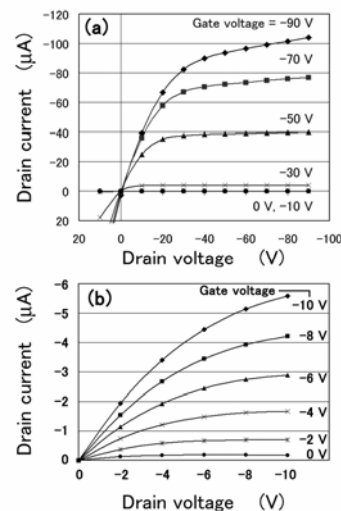


FIG. 6 Drain current versus drain voltage characteristics of a p-type pentacene OFET fabricated on the  $\text{Ta}_2\text{O}_5/\text{Ta}$  gate as a function of the gate voltage. (a) high voltage operation, (b) low voltage operation.

can also work as the gate capacitor of an n-type OFET. Under the n-type working conditions, a positive bias voltage is applied between the gate and source electrodes, so the gate leak current is smaller than that of the p-type pentacene FET. The gate current leak, however, occurs when the gate voltage (positive against source) is small and the drain voltage (positive against source) is large, because under this condition, the gate potential is effectively negative against the drain potential. This phenomenon is clearly observed in Fig. 7 for the gate voltage less than 30 V. For the drain voltage less than 40 V, however, typical FET characteristics are observed.

The mobility of this C<sub>60</sub> OFET was 0.007 cm<sup>2</sup>/Vs in the linear region, which is far smaller than that reported in the literature<sup>18</sup> or that fabricated on a SiO<sub>2</sub>/Si gate by ourselves (approximately 0.5 cm<sup>2</sup>/Vs). The poorer performance seems to come from the low quality of the C<sub>60</sub> film grown on the anodized Ta<sub>2</sub>O<sub>5</sub> surface, which was revealed by the AFM image shown in Fig. 8. Compared with the pentacene film shown in Fig. 5, the C<sub>60</sub> domains are far smaller, and there are quite a large number of grain boundaries. These defects in the active channel are considered to reduce the drain-source current and make the mobility worse. We consider that the growth conditions (growth rate, substrate temperature) should be optimized together with the surface modification by covering the Ta<sub>2</sub>O<sub>5</sub> surface with an organic self-assembled monolayer or a Langmuir-Blodgett film. If the quality of the C<sub>60</sub> film is improved and good junctions between the C<sub>60</sub> film and source/drain electrodes are fabricated, the ideal carrier injection of one e<sup>-</sup> / 1.5 C<sub>60</sub> occurs for the electric field of 5 MV/cm. The semiconductor-metal transition, which has been really observed in the chemically doped C<sub>60</sub> films,<sup>19</sup> is expected to occur in this physically electron doped C<sub>60</sub> film.

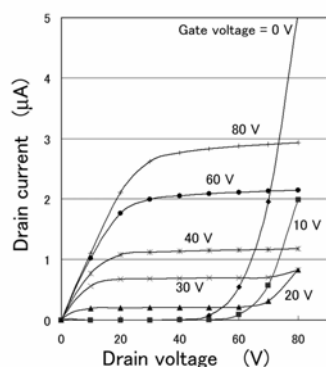


FIG. 7 Drain current versus drain voltage characteristics of an n-type C<sub>60</sub> OFET fabricated on the Ta<sub>2</sub>O<sub>5</sub>/Ta gate as a function of the gate voltage.

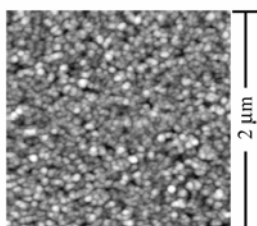


FIG. 8 An AFM image of a C<sub>60</sub> film grown on the anodized Ta<sub>2</sub>O<sub>5</sub> surface at room temperature.

#### IV. CONCLUSIONS

Electrolytically polished surfaces of Ta sheets were anodized in an aqueous KI solution to form Ta<sub>2</sub>O<sub>5</sub> films. Organic field effect transistors (OFETs) were fabricated on the Ta<sub>2</sub>O<sub>5</sub>/Ta with a bottom gate configuration. The anodized Ta<sub>2</sub>O<sub>5</sub> films showed a dielectric strength as high as 5 MV/cm when a positive bias voltage was applied to the gate electrode. A p-type pentacene OFET fabricated on this bottom gate showed a good field-effect mobility of 0.35 cm<sup>2</sup>/Vs, overcoming the unfavorable gate polarity. An n-type C<sub>60</sub> OFET fabricated on the Ta<sub>2</sub>O<sub>5</sub>/Ta gate, however, showed a poor mobility, 0.007 cm<sup>2</sup>/Vs, due to the poor quality of the grown film. It was confirmed that the preparation of a highly flat surface preceding the anodization is essential for achieving a high quality Ta<sub>2</sub>O<sub>5</sub>/Ta gate.

#### References

- <sup>1</sup>A. Tsumura, H. Koezuka, and T. Ando, *Appl. Phys. Lett.* **49**, 1210 (1986).
- <sup>2</sup>C.D. Dimitrakopoulos and P.R.L. Malenfant, *Adv. Mater.* **14**, 99 (2002).
- <sup>3</sup>J. C. Scott, *J. Vac. Sci. Technol. A* **21**, 521 (2003).
- <sup>4</sup>B.H. Hamadani and D. Natelson, *J. Appl. Phys.* **97**, 0645058 (2005).
- <sup>5</sup>C.D. Dimitrakopoulos, S. Purushothanman, J. Kymissis, A. Callegari, and J.M. Shaw, *Science* **283**, 822 (1999).
- <sup>6</sup>J. Tate, J.A. Rogers, C.D. Jones, B. Vyas, D.W. Murphy, W. Li, Z. Bao, R. E. Slusher, A. Dodabalapur, and H.E. Katz, *Langmuir* **16**, 6054 (2000).
- <sup>7</sup>Y. Ino, Y. Inoue, Y. Fujisaki, H. Fujitaka, H. Sato, M. Kawakita, S. Tokito, and H. Kikuchi, *Jpn. J. Appl. Phys.*, Part 1 **42**, 299 (2003).
- <sup>8</sup>Y. Fujisaki, Y. Inoue, T. Kurita, S. Tokito, H. Fujisaki, and H. Kikuchi, *Jpn. J. Appl. Phys.*, Part 1 **43**, 372 (2004).
- <sup>9</sup>C. Bartic, H. Jansen, A. Campitelli, and S. Borghs, *Org. Electronics* **3**, 65 (2002).
- <sup>10</sup>H. Sakai, Y. Furukawa, E. Fujiwara, and H. Tada, *Chem. Lett.* **33**, 1172 (2004).
- <sup>11</sup>G.S. Oehriein, *J. Appl. Phys.* **59**, 1587 (1986).
- <sup>12</sup>D.A. Vermilyea, *Acta Metall.* **1**, 282 (1953).
- <sup>13</sup>J.J. Randall, JR., W.J. Bernard, and R.R. Wilkinson, *Electrochem. Acta* **10**, 183 (1965).
- <sup>14</sup>Q. Lu, S. Mato, P. Skeldon, G.E. Thompson, D. Masheder, H. Habazaki, and K. Shimizu, *Electrochem. Acta* **47**, 2761 (2002).
- <sup>15</sup>H. Masuda and K. Fukuda, *Science* **268**, 1466 (1995).
- <sup>16</sup>I. Sieber, B. Kannan, and P. Schmuki, *Electrochem. Solid-State Lett.* **8**, J10 (2005).
- <sup>17</sup>C.D. Dimitrakopoulos, A.R. Brown, and A. Pomp, *J. Appl. Phys.* **80**, 2501 (1996).
- <sup>18</sup>S. Kobayashi, T. Takenobu, S. Mori, A. Fujiwara, and Y. Iwasa, *Appl. Phys. Lett.* **82**, 4581 (2003).
- <sup>19</sup>R.C. Haddon, A.F. Hebard, M.J. Rosseinsky, D.W. Murphy, S.J. Duclos, K.B. Lyons, B. Miller, J.M. Rosamilia, R.M. Fleming, A.R. Kortan, S.H. Glarum, A.V. Makhija, A.J. Muller, R.H. Eick, S.M. Zahurak, R. Tycko, G. Dabbagh, and F.A. Thiel, *Nature (London)* **350**, 320 (1991).